Overtone Spectrum of Stannane: Experiment and Theoretical Analysis

Marjo Halonen, Lauri Halonen,*

Department of Physical Chemistry, University of Helsinki, Meritullinkatu 1 C, SF-00170 Helsinki, Finland

Hans Bürger, and Silvia Sommer

FB 9—Anorganische Chemie, Universität-Gesamthochschule, D-5600 Wuppertal, Federal Republic of Germany
(Received: October 18, 1989; In Final Form: January 10, 1990)

The infrared spectrum of monoisotopic species of stannane, $^{116}SnH_4$, has been measured with medium resolution in the region 1900–6000 cm^{-1}. The bands observed include the infrared-active stretching fundamental band and the first and second stretching overtone bands. The vibrational term values of the observed bands are analyzed with a local mode model where anharmonic bond oscillators are coupled through bilinear kinetic energy and potential energy terms. The potential energy parameters are optimized with the nonlinear least-squares method using observed vibrational term values as data. The observed infrared absorption intensities are analyzed with a bond dipole model.

Introduction

Highly excited vibrational states of tetrahedral molecules have attracted a lot of interest in recent years.[1-11] This is due to both experimental and theoretical developments in the area of overtone spectroscopy. Besides the conventional infrared and Raman techniques, it has become possible to use Fourier infrared interferometers[12-14] and various laser techniques such as dye lasers with photoacoustic detection methods,[15] infrared–infrared double resonance experiments,[4] and microwave-detected microwave optical double resonance experiments[16] to probe the excited states of polyatomic molecules. The theoretical work in this area concentrates on the development and use of both local mode models[1-3,11] and conventional approaches with anharmonic expansions on diagonal and Darling–Dennison resonance operators off diagonal.[7] The purpose of this work is to understand experimental energy level structures and to derive potential energy surfaces. These results can then be used to understand various dynamical aspects such as energy transfer between different degrees of freedom in polyatomic molecules.

The interest in the stretching vibrational overtone spectrum of stannane lies in the local mode energy level character. The small observed energy level separation, 2.3 cm^{-1} in $^{116}SnH_4$, of the symmetric (A_1) and triply degenerate antisymmetric (F_2) stretching fundamentals suggests that stannane is close to the local mode limit.[17] Thus the local mode model should be particularly suitable to analyze the experimental stretching vibrational term values as some earlier work on other tetrahedral molecules indicates.[2,3,9,10] It would also be of interest to see how well a simple bond dipole model together with the local mode model produces experimental infrared absorption intensities for transitions from the ground state to the excited vibrational states.

Experimental data of excited stretching vibrational states of stannane are scarce. Apart from fundamentals and the first stretching overtone of SnH_4 there are no other experimental data available.[17,18] Only in the case of a high-resolution study of the stretching fundamental ν_1/ν_3 pair the isotope shifts due to major isotopic species of Sn ($^{116}SnH_4$, 14.5%; $^{117}SnH_4$, 7.7%; $^{118}SnH_4$, 24.2%; $^{119}SnH_4$, 8.6%; $^{120}SnH_4$, 32.6%; $^{122}SnH_4$, 4.6%; and $^{124}SnH_4$, 5.8%) have been observed.[17]

In this study the infrared spectrum of monoisotopic species of stannane, $^{116}SnH_4$, is measured in the stretching fundamental region and in the overtone region up to 6000 cm^{-1}. Besides the fundamentals and the first stretching overtone [$(2000,A_1/F_2)$ in the local mode notation[1,2]], which have been seen before only in a natural sample of SnH_4, the second overtone band $(3000,A_1/F_2)$ is observed. The relative intensities of the stretching vibrational bands are measured for the first time. The observed experimental results are used with a simple local mode model and a bond dipole model to obtain a stretching vibrational potential energy surface and a dipole moment function for stannane.

Experimental Method

Monoisotopic $^{116}SnH_4$ was prepared by letting a solution containing $SnCl_6^{2-}$ (1 mg of Sn/mL) react with an aqueous solution of $NaBH_4$ (3%) under vacuum (50–80 mbar). The $SnCl_6^{2-}$ solution was made by dissolving ^{116}Sn (98% ^{116}Sn; Oak Ridge National Laboratory) in an aqueous HCl/HNO_3 (50:1) mixture. Gaseous $^{116}SnH_4$ evolved was collected at a temperature of −196 °C and purified by repeated fractional condensation using a standard vacuum line. The yield obtained is about 90%. Only small amounts of CO_2 and N_2O were found as contaminants.

FTIR spectra were recorded with a Nicolet 7199 instrument. In the case of $(1000,F_2)$ and $(2000,F_2)$ bands the spectrometer

(1) Child, M. S.; Halonen, L. *Adv. Chem. Phys.* **1984**, *57*, 1.
(2) Halonen, L.; Child, M. S. *Mol. Phys.* **1982**, *46*, 239.
(3) Abram, I.; De Martino, A.; Frey, R. *J. Chem. Phys.* **1982**, *76*, 5727. Chevalier, M.; De Martino, A. *J. Chem. Phys.* **1989**, *90*, 2077.
(4) De Martino, A.; Frey, R.; Pradere, F. *Chem. Phys. Lett.* **1983**, *95*, 200. De Martino, A.; Frey, R.; Pradere, F. *Chem. Phys. Lett.* **1983**, *100*, 329. De Martino, A.; Frey, R.; Pradere, F. *Chem. Phys. Lett.* **1984**, *111*, 113. De Martino, A.; Frey, R.; Pradere, F. *Mol. Phys.* **1985**, *55*, 731.
(5) McKean, D. C.; Morrisson, A. R.; Kelly, M. I. *Chem. Phys. Lett.* **1984**, *109*, 347.
(6) Bernheim, R. A.; Lampe, F. W.; O'Keefe, J. F.; Qualey, J. R., III *J. Chem. Phys.* **1984**, *80*, 5906. Bernheim, R. A.; Allbee, D. C.; Lampe, F. W.; O'Keefe, J. F.; Qualey, J. R., III *J. Phys. Chem.* **1988**, *92*, 1850.
(7) Mills, I. M.; Robiette, A. G. *Mol. Phys.* **1985**, *56*, 743.
(8) Halonen, L. *J. Mol. Spectrosc.* **1986**, *120*, 175.
(9) Halonen, L.; Child, M. S. *Comput. Phys. Commun.* **1988**, *51*, 173.
(10) Halonen, L. *J. Phys. Chem.* **1989**, *93*, 631.
(11) Halonen, L. *J. Phys. Chem.* **1989**, *93*, 3386.
(12) Griffiths, P. R.; De Haseth, J. A. *Fourier Transform Infrared Spectrometry*; Wiley: New York, 1986.
(13) Baggott, J. E.; Clase, H. J.; Mills, I. M. *Spectrochim. Acta* **1986**, *42A*, 319. Baggott, J. E.; Law, D. W.; Lightfoot, P. D.; Mills, I. M. *J. Chem. Phys.* **1986**, *85*, 5414.
(14) Duncan, J. L.; Nivellini, G. D.; Tullini, F. *J. Mol. Spectrosc.* **1986**, *118*, 145. Duncan, J. L.; Ferguson, A. M.; Mathews, S. *J. Chem. Phys.* **1989**, *91*, 783.
(15) Long, M. E.; Swofford, R. L.; Albrecht, A. C. *Science (Washington, D.C.)* **1976**, *191*, 183. Scherer, G. J.; Lehmann, K. K.; Klemperer, W. *J. Chem. Phys.* **1983**, *78*, 2817. *Ibid.* **1984**, *81*, 5319. Wong, J. S.; Green, W. H., Jr.; Cheng, C.; Moore, C. B. *J. Chem. Phys.* **1987**, *86*, 5994.
(16) Lehmann, K. K.; Coy, S. L. *J. Chem. Phys.* **1984**, *81*, 3744. Coy, S. L.; Lehmann, K. K. *Spectrochim. Acta* **1989**, *45A*, 47.
(17) Jörissen, L.; Ohshima, Y.; Matsumoto, Y.; Takami, M.; Kuchitsu, K. *J. Chem. Phys.* **1989**, *90*, 2109.
(18) Kattenberg, H. W.; Oskam, A. *J. Mol. Spectrosc.* **1974**, *51*, 377.

0022-3654/90/2094-5222$02.50/0

was equipped with a KBr/Ge beam splitter and an MCT detector. An infrared gas cell with an optical path length of 17.7 cm was employed. Sample pressures ranged from 1 to 70 mbar. The optical resolution was about 0.5 cm^{-1}. A spectrum of the (2000,F_2) band was also obtained with a medium resolution of 0.12 cm^{-1} employing an InSb detector and an optical filter that eliminates radiation above 3900 cm^{-1} and below 2900 cm^{-1}. The medium-resolution spectrum was calibrated with known H_2O lines.[19] The (2000,F_2) and (3000,F_2) bands were also recorded simultaneously with a Wilks multireflection cell adjusted to an optical path length of 21.75 m. The sample pressure used in this experiment was 7 mbar measured with an MKS Baratron pressure gauge. A Si:CaF_2 beam splitter and an InSb detector were used. The resolution was adjusted to 1 cm^{-1}. Both of the stretching overtone bands are shown with the same transmission scale in Figure 1. A better resolved spectrum (0.05 cm^{-1}) of $^{116}SnH_4$ in the stretching fundamental region is shown elsewhere.[20]

Relative intensities were determined by comparing areas of Q branches and P and R clusters recorded with a resolution of 1 cm^{-1}. For the stronger band [(1000) with respect to (2000) and (2000) with respect to (3000)] the product path length times pressure was adjusted to produce a band with the same absorbance as the weaker band with which it was compared. For confirmation this procedure was repeated to measure the relative intensities of the (1000) and (2000) bands with a Perkin-Elmer 580B grating spectrometer. The resolution of this measurement was such (about 5 cm^{-1}) that only the envelopes of P, Q, and R branches could be produced.

Theoretical Model

Curvilinear internal displacement coordinates $\mathbf{r}$ and their conjugate momentum operators $\mathbf{p}_r$ can be used to express the vibrational quantum mechanical Hamiltonian as[21,22]

$$H = \tfrac{1}{2}\mathbf{p}_r^{\dagger}\mathbf{g}(\mathbf{r})\mathbf{p}_r + V'(\mathbf{r}) + V(\mathbf{r}) \quad (1)$$

where $\mathbf{g}(\mathbf{r})$ is a matrix (Wilson's $\mathbf{g}$ matrix) whose elements are functions of atomic masses and internal coordinates.[23] $V'(\mathbf{r})$ is a small kinetic energy term that does not involve momentum operators. $V(\mathbf{r})$ is the usual potential energy function expressed in terms of internal displacement coordinates.

In the present application we are dealing with stretching vibrations only. In constructing a suitable Hamiltonian for our purposes we constrain the angle bend displacement coordinates to zero. Thus the corresponding momentum operators disappear and the Hamiltonian takes the simple form[2,8-10]

$$H = \tfrac{1}{2}g_{rr}\sum_{i=1}^{4}p_i^2 + g_{rr'}\sum_{i<j}p_ip_j + V(\mathbf{r}) \quad (2)$$

where the small purely quantum mechanical term $V'(r_1,r_2,r_3,r_4)$ is omitted. $p_j = -i\hbar(\partial/\partial r_j)$ is the momentum conjugate to the bond displacement coordinate r_j of the jth bond. The kinetic energy coefficients g_{rr} and $g_{rr'}$ are given as

$$g_{rr} = 1/m_{Sn} + 1/m_H = 1/\mu \quad (3)$$

and

$$g_{rr'} = (\cos\alpha_e)/m_{Sn} = -1/(3m_{Sn}) \quad (4)$$

where m_{Sn} and m_H are the masses of the Sn and H atoms, respectively, and α_e is the equilibrium value of the valence tetrahedral angle. It has been found in the past that the Morse potential energy function describes adequately the stretching vibrational states of polyatomic molecules up to fairly high vibrational excitation.[1,24] Therefore also in this work Morse functions are used to describe the four bond oscillators which are coupled with each other by potential energy cross terms (and by kinetic energy cross terms; see eq 2). Two different kinds of potential energy cross terms are used. In model I the potential energy function adopted is

$$V = D_e\sum_{i=1}^{4}y_i^2 + f_{rr'}\sum_{i<j}r_ir_j \quad (5)$$

and in model II

$$V = D_e\sum_{i=1}^{4}y_i^2 + f_{rr'}a^{-2}\sum_{i<j}y_iy_j \quad (6)$$

where $y_i = 1 - \exp(-ar_i)$ is the Morse variable. The Morse dissociation energy D_e, the Morse parameter a, and the coupling force constant $f_{rr'} = (\partial^2V/(\partial r_i\,\partial r_j))_e$ $(i \neq j)$ are potential energy parameters. The potential energy function of model I is obtained from the potential energy function of model II by expanding the y_i variables in the potential energy coupling term (the term in $f_{rr'}$) and retaining the first term in the expansion. The advantage in the use of model II is the correct asymptotic limit of the potential energy function at large stretching displacements.

The eigenvalues of the Hamiltonian given in eq 2 are best obtained variationally by employing products of Morse oscillator eigenfunctions ($|n_1n_2n_3n_4\rangle = |n_1\rangle|n_2\rangle|n_3\rangle|n_4\rangle$), which are chosen to be consistent with the Morse parameter a and the dissociation energy D_e. This procedure uses analytic expressions for the Hamiltonian matrix elements.[1,2,8,9,25,26] The Hamiltonian matrices are factorized by employing symmetrized basis sets as described in detail in recent papers.[9,27] The potential energy parameters a, D_e, and $f_{rr'}$ are optimized with the nonlinear least-squares method[9] using experimental stretching vibrational term values as data.

The infrared absorption intensities for transitions from the ground state to excited F_2 states are calculated by use of a bond dipole model

$$\mu(\mathbf{R}) = \sum_{i=1}^{4}\mu(R_i)\mathbf{e}_i \quad (7)$$

where $\mathbf{e}_i$ is a unit vector along the ith bond and R_i is the instantaneous bond length of the ith bond. The form for $\mu(R_i)$ used in this work takes the form[28,29]

$$\mu(R_i) = \mu_0R_ie^{-R_i/R^*} = \mu_0R_ie^{-a\lambda R_i} \quad (8)$$

where μ_0 and R^* (or λ) are adjustable parameters. a is the Morse parameter appearing in the vibrational Hamiltonian. μ_0 is not relevant in the present application where only relative intensity information is available. Although the dipole function adopted possesses correct limits as $R_i \to 0$ or $R_i \to \infty$, it must be regarded just as an empirical function without a deeper physical inter-

TABLE I: Potential Energy Parameters for Stannane[a]

parameter	model I	model II
a/Å^{-1}	1.334 294 (270)	1.334 166 (110)
D_e/aJ	0.638 908 6 (2400)	0.639 265 9 (990)
$f_{rr'}$/aJ Å^{-2}	0.007 466 43 (1500)	0.007 943 81 (660)
f_{rr}/aJ Å^{-2}	2.275[b]	2.276[b]
f_{rrr}/aJ Å^{-3}	−9.106[b]	−9.109[b]
f_{rrrr}/aJ Å^{-4}	28.35[b]	28.36[b]

[a] The uncertainties given in parentheses are one standard error in the least significant digit. 1 aJ = 10^{-18} J and 1 Å = 10^{-10} m. [b] Calculated from a and D_e (see text).

(19) Flaud, J. M.; Camy-Peyret, C.; Toth, R. A. *International Tables of Selected Constants*; Pergamon: Oxford, 1981; Vol. 19.
(20) Bürger, H.; Rahner, A. In *Vibrational Spectra and Structure*; Durig, J. R., Ed.; Elsevier: Amsterdam, 1989; Vol. 18, in press.
(21) Pickett, H. M. *J. Chem. Phys.* **1972**, *56*, 1715. Meyer, R.; Günthard, Hs. H. *J. Chem. Phys.* **1968**, *49*, 1510.
(22) Halonen, L.; Carrington, T., Jr. *J. Chem. Phys.* **1988**, *88*, 4171.
(23) Wilson, E. B.; Decius, J. C.; Cross, P. C. *Molecular Vibrations*; McGraw-Hill: New York, 1955.
(24) Henry, B. R. In *Vibrational Spectra and Structure*; Durig, J. R., Ed.; Elsevier: New York, 1981; Vol. 10.
(25) Sage, M. L. *Chem. Phys.* **1978**, *35*, 375. Sage, M. L.; Williams, J. A., III *J. Chem. Phys.* **1983**, *78*, 1348. Carney, G. D.; Porter, R. N. *J. Chem. Phys.* **1976**, *65*, 3547. Carney, G. D.; Sprandel, L. L.; Kern, C. W. *Adv. Chem. Phys.* **1978**, *37*, 305.
(26) Kauppi, E.; Halonen, L. *J. Chem. Phys.* **1989**, *90*, 6980.
(27) Halonen, L.; Child, M. S. *J. Chem. Phys.* **1983**, *79*, 559.
(28) Mecke, R. *Z. Electrochem.* **1950**, *54*, 38.
(29) Schek, I.; Jortner, J.; Sage, M. L. *Chem. Phys. Lett.* **1979**, *64*, 209.

TABLE II: Input Data and Fits in the Potential Parameter Optimization and Intensity Calculations[a]

	ν_{obsd}/cm^{-1}	$\Delta\nu/cm^{-1}$	model I (o − c)/cm^{-1}	model II (o − c)/cm^{-1}	model II I_{calc}	I_{obs}
			$^{116}SnH_4$			
1000 F_2	1905.8349	0.5	−0.029	−0.023	[1.0][b]	[1.0][b]
1000 A_1	1908.1002	0.5	0.002	0.003		
2000 F_2	3752.66	1.0	−0.158	−0.073	0.17×10^{-1}	0.25×10^{-1}
2000 A_1	3752.75	1.0	0.212	−0.015		
3000 F_2	5539.05	1.0	−0.011	0.015	0.26×10^{-3}	0.13×10^{-3}
3000 A_1	5539.05	1.0	−0.007	0.014		
			$^{117}SnH_4$			
1000 F_2	1905.7574	0.5	−0.015	−0.010		
1000 A_1	1908.1002	0.5	0.001	0.002		
			$^{118}SnH_4$			
1000 F_2	1905.6814	0.5	−0.002	0.004		
1000 A_1	1908.1013	0.5	0.001	0.002		
			$^{119}SnH_4$			
1000 F_2	1905.6067	0.5	0.011	0.017		
1000 A_1	1908.1003	0.5	−0.001	0.000		
			$^{120}SnH_4$			
1000 F_2	1905.5331	0.5	0.024	0.029		
1000 A_1	1908.0991	0.5	−0.004	−0.002		

[a] $\Delta\nu$ is the uncertainty used in the refinement. The corresponding weight is calculated as $w = 1/(\Delta\nu)^2$. o − c denotes observed minus calculated wavenumber. I_{obs} and I_{calc} are observed and calculated intensities, respectively. Stretching fundamental wavenumbers are taken from ref 17. All other experimental data are from this work. [b] Scaled value.

pretation. One advantage in its use is the fact that analytic matrix elements are available as given in the following equations:[26,29]

$$\langle n+j|R_i e^{-a\lambda R_i}|n\rangle = a^{-1}k^{-\lambda}e^{-a\lambda R_e}\left[(aR_e + \ln k)\langle n+j|z^\lambda|n\rangle - \frac{d}{d\lambda}\langle n+j|z^\lambda|n\rangle\right] \quad (9)$$

where

$$z = k\exp[-a(R_i - R_e)] \quad (10)$$

$$k = \frac{2}{a\hbar}(2D_e\mu)^{1/2} \quad (11)$$

$$\langle n+j|z^\lambda|n\rangle = a^{-1}N_{n+j}N_n\sum_{l=0}^{n}\binom{l-\lambda}{l+j}\binom{j+l-\lambda}{l}\frac{\Gamma(k+\lambda-n-j-l-1)}{(n-l)!} \quad (12)$$

$$\frac{d}{d\lambda}\langle n+j|z^\lambda|n\rangle = a^{-1}N_{n+j}N_n\sum_{l=0}^{n}\left\{[-\Phi(l-\lambda+1) - \Phi(j+l-\lambda+1) + \Phi(k+\lambda-n-j-l-1) + \Phi(-\lambda-j+1) + \Phi(j-\lambda+1)] \times \binom{l-\lambda}{l+j}\binom{j+l-\lambda}{l}\frac{\Gamma(k+\lambda-n-j-l-1)}{(n-l)!}\right\} \quad (13)$$

and

$$N_n = \left[\frac{an!(k-2n-1)}{\Gamma(k-n)}\right]^{1/2} \quad (14)$$

R_e is the equilibrium bond length. $\Gamma(z)$ and $\Phi(z) = d\ln\Gamma(z)/dz$ are gamma and digamma functions, respectively.[30] n is the vibrational quantum number and j is an integer ≥0. The infrared absorption intensities are then calculated as[23]

$$I_{f0} = C\nu\sum_{\xi=x,y,z}\langle f|\mu(\mathbf{R})\cdot\mathbf{e}_\xi|0\rangle^2 \quad (15)$$

where the ground-state wave function $|0\rangle$ and the upper-state wave function $\langle f|$ are obtained as eigenvectors by diagonalizing the A_1 and F_2 Hamiltonian matrices, respectively. C is a constant, ν is the wavenumber of the transition in question, and $\mathbf{e}_\xi$ is a unit vector along the x, y, or z principal axis.

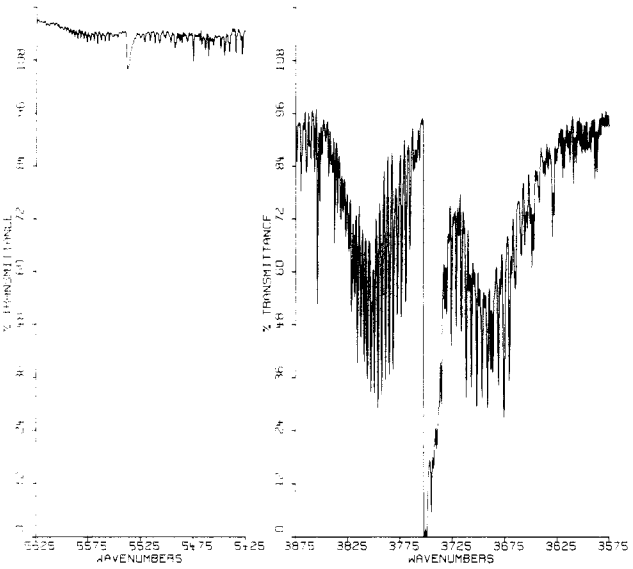

Figure 1. (3000,A_1/F_2) and (2000,A_1/F_2) infrared bands of $^{116}SnH_4$.

Results for Stannane

Stannane is a particularly suitable candidate for the local mode analyses because the bending fundamentals [$\nu_2(E) = 753.3$ cm^{-1} and $\nu_4(F_2) = 680.9$ cm^{-1} in $^{116}SnH_4$] are much lower in wavenumber than the stretching fundamentals [$\nu_1(A_1) = 1908.1$ cm^{-1} and $\nu_3(F_2) = 1905.8$ cm^{-1} in $^{116}SnH_4$].[17,31] Fermi resonances between stretching and bending states common in many molecules are insignificant in stannane.

The stretching fundamental wavenumbers of five isotopic species of stannane ($^{116}SnH_4$, $^{117}SnH_4$, $^{118}SnH_4$, $^{119}SnH_4$, and $^{120}SnH_4$) are taken from a previous high-resolution study.[17] In this work we have measured the first and the second stretching overtone bands of $^{116}SnH_4$. Only the transition to the lowest local mode pair within each overtone manifold (a set of levels for which $v_{stretch}$ is constant) is observed. Thus just transitions to the almost

(30) Abramowitch, M.; Stegun, I. A. *Handbook of Mathematical Functions*; Dover: New York, 1965.

(31) Ohshima, Y.; Matsumoto, Y.; Takami, M.; Yamamoto, S.; Kuchitsu, K. *J. Chem. Phys.* **1987**, *87*, 5141.

degenerate local mode pair (2000,A_1) and (2000,F_2) and to the almost degenerate pair (3000,A_1) and (3000,F_2) are observed as is seen from Figure 1. The (2000,A_1/F_2) band system appears as a symmetric-top parallel band in our medium-resolution Nicolet spectrum. This is typical of a spherical-top molecule close to the local mode limit.[32,33] In fact we have determined the band origin $\nu(2000,A_1/F_2) = 3752.681 \pm 0.010$ cm^{-1} by using the symmetric-top formula for infrared transitions.[34] This compares well with $\nu(2000,A_1) = 3752.75$ cm^{-1} and $\nu(2000,F_2) = 3752.66$ cm^{-1} obtained from a preliminary analysis of a high-resolution IR spectrum of stannane going on in our laboratories. In the case of the (3000,A_1/F_2) band system the quality of our spectra is such that we have only performed a polynomial fit of rotational clusters and we have corrected roughly the error made by neglecting the cluster structure. For the band center we obtain an estimate $\nu(3000,A_1/F_2) = 5538.4 \pm 0.3$ cm^{-1}. This may be compared with the wavenumber 5539.05 ± 0.02 cm^{-1} obtained from a preliminary rotational analysis of the Doppler limited high-resolution FT spectrum of $^{116}SnH_4$ going on in our laboratories. The discrepancy between the last two different measurements may seem large, but in fact the agreement is acceptable bearing in mind that the uncertainties given are only standard errors. The band centers obtained from the two different measurements are within three standard errors which is a more crucial test. A detailed analysis of the high-resolution spectra of these bands might change these estimates slightly, but it is unlikely that more accurate vibrational term values would have any significant effect on the results presented below. We have determined the intensity ratio of the fundamental stretching bands and the first stretching overtone to be 40 ± 5 and the intensity ratio of the first and second stretching overtones to be 195 ± 50. The uncertainties given are somewhat conservative due to experimental difficulties in obtaining these intensity ratios accurately.

The potential energy parameters optimized by the nonlinear least-squares method are given in Table I for both models. This table also includes the stretching force constants $f_{rr} = (\partial^2 V/\partial r_i^2)_e = 2a^2 D_e$, $f_{rrr} = (\partial^3 V/\partial r_i^3)_e = -3a f_{rr}$, and $f_{rrrr} = (\partial^4 V/\partial r_i^4)_e = 7a^2 f_{rr}$. The input data used in the potential parameter optimization and the fits obtained are given in Table II. The available experimental stretching fundamental $\nu_3 = 1367.5$ cm^{-1} of SnD_4 was not included in the data set of the least-squares calculation. The resolution of that study is such that the isotope shifts due to different tin isotopes are not observed.[35] Four times higher weights were used for fundamentals than for overtones (see Table II). The basis set sizes were such that all basis functions $v_{stretch} = \sum_{i=1}^{4} n_i \leq 7$ were included for $^{116}SnH_4$ and all basis functions $v_{stretch} \leq 5$ were included for other isotopic species. Test calculations show that the basis sets used give a good convergence. The standard deviations of the fits, 0.047 cm^{-1} for potential model I and 0.020 cm^{-1} for potential model II, show the excellent agreement between theory and the model adopted. Model II produces slightly better results, and it also produces correctly the order of the (2000) states unlike model I (see Table II).

The observed and calculated infrared absorption intensities are given in Table II. The dipole moment function parameter $R^* = 0.85$ Å and the SnH bond length $R_e = 1.7108$ Å (taken from ref 35) were used in the intensity calculations. The observed intensities are reasonably well reproduced in light of the fairly large uncertainties attached to the measured relative intensities.

Table III contains all calculated vibrational term values of $^{116}SnH_4$ and $^{116}SnD_4$ produced with model II up to $v_{stretch} = 5$ and in wavenumber the lowest F_2 components in each overtone manifold up to $v_{stretch} = 10$. All basis functions up to $v_{stretch} = 12$ are included in these calculations. The calculated energy levels of both isotopic species show close local mode degeneracies with small splittings of a few wavenumbers at all excitation levels. This is typical of molecules close to the local mode limit.[1,2,36] The calculated term values should be helpful for prediction purposes, for example, in dye laser studies and in recent studies of infrared–infrared double resonance type.[4] The intensity calculations for the transitions from the ground state to the F_2 states show that in a particular overtone manifold the transitions to the lowest F_2 component carries several orders of magnitude more intensity than the transitions to the other F_2 components. The calculated relative

TABLE III: Calculated Term Values (cm^{-1}) for $^{116}SnH_4$ and $^{116}SnD_4$ Measured from the Ground Vibrational State

			model II	
v			$^{116}SnH_4$	$^{116}SnD_4$
1	1000	F_2	1905.9	1368.1
		A_1	1908.1	1362.1
2	2000	F_2	3752.7	2702.7
		A_1	3752.8	2701.8
	1100	E	3811.9	2736.4
		F_2	3813.1	2733.6
		A_1	3815.3	2728.3
3	3000	F_2	5539.0	4008.6
		A_1	5539.0	4008.5
	2100	F_1	5658.0	4074.2
		F_2	5658.8	4065.8
		E	5660.1	4068.4
		F_2	5661.0	4072.0
		A_1	5661.7	4062.5
	1110	F_2	5719.4	4102.2
		A_1	5721.7	4097.2
4	4000	F_2	7265.3	5284.3
		A_1	7265.3	5284.3
	3100	F_1	7445.5	5377.4
		F_2	7445.5	5372.4
		E	7445.5	5376.3
		F_2	7447.2	5376.7
		A_1	7447.2	5371.6
	2200	E	7506.4	5407.0
		F_2	7506.4	5406.6
		A_1	7506.4	5405.7
	2110	F_1	7565.0	5441.3
		E	7565.1	5441.4
		F_2	7566.4	5432.2
		F_2	7568.6	5437.8
		A_1	7569.9	5428.3
	1111	A_1	7627.0	5468.5
5	5000	F_2	8931.4	6529.7
		A_1	8931.4	6529.7
	4100	F_1	9171.9	6652.8
		F_2	9171.9	6648.2
		E	9171.9	6652.7
		F_2	9173.6	6652.8
		A_1	9173.6	6648.2
	3200	F_1	9291.5	6716.9
		F_2	9291.6	6707.8
		E	9294.6	6708.1
		F_2	9294.6	6716.5
		A_1	9294.6	6707.4
	3110	F_1	9352.7	6744.4
		E	9352.7	6744.4
		F_2	9352.8	6740.0
		F_2	9354.4	6742.9
		A_1	9354.5	6738.4
	2210	F_1	9412.0	6778.2
		F_2	9412.7	6769.6
		E	9413.2	6775.5
		F_2	9415.7	6776.3
		A_1	9416.4	6766.7
	2111	F_2	9472.9	6807.4
		A_1	9477.2	6796.8
6	6000	F_2	10537.5	7744.8
7	7000	F_2	12083.5	8929.5
8	8000	F_2	13569.5	10084.0
9	9000	F_2	14995.4	11208.1
10	10000	F_2	16361.3	12302.0

(32) Halonen, L.; Robiette, A. G. *J. Chem. Phys.* **1986**, *84*, 6861. Halonen, L. *J. Chem. Phys.* **1987**, *86*, 588.
(33) Zhu, Q.; Thrush, B. A.; Robiette, A. G. *Chem. Phys. Lett.* **1988**, *150*, 181.
(34) Herzberg, G. *Infrared and Raman Spectra*; Van Nostrand: New York, 1945.
(35) Child, M. S.; Lawton, R. T. *Faraday Discuss. Chem. Soc.* **1981**, *71*, 273. Mortensen, O. S.; Henry, B. R.; Mohammadi, M. A. *J. Chem. Phys.* **1981**, *75*, 4800.

intensities of $^{116}SnH_4$ for the (1000,F_2), (2000,F_2), ..., (10000,F_2) bands are 1.0, 0.017, 0.26×10^{-3}, 0.14×10^{-5}, 0.19×10^{-6}, 0.13×10^{-6}, 0.37×10^{-7}, 0.90×10^{-8}, 0.21×10^{-8}, and 0.51×10^{-9}, respectively. We also note that in the case of weaker transitions from the ground state to F_2 states within a particular overtone manifold it would be a poor approximation to assume that the ground-state wave function is a pure $|0000\rangle = |0\rangle|0\rangle|0\rangle|0\rangle$ state as was assumed in some earlier work.[2,9]

Conclusion

The simple local mode model used produces the experimental vibrational term values well. It is of course true that the experimental data set is limited, but the experience with SiH_4 and GeH_4 suggests that the predicted higher vibrational term values of stannane would be quite accurate and can be used to assign more spectra in the future.[2,9,10] Model II of the two potential models used seems to work a bit better. It also has the advantage that is possesses realistic asymptotic limits at large SnH stretching amplitudes. Thus this model might be more suitable for molecular dynamics studies.

The experimental intensities are less strikingly well produced by the model. This might be due to the oversimple form of the bond dipole model. First, no cross terms are included in the dipole moment function. Second, since it is just an empirical function, the non cross terms included might be too simple. One must also be aware of the experimental difficulties in measuring intensities accurately. Thus we think that the agreement between measured and calculated relative intensities is satisfactory, keeping in mind the uncertainties arriving from both the experiment and the limitations of the model. It would certainly be worth measuring higher overtone states with intensities in order to be able to determine the dipole moment function more accurately.

The medium-resolution infrared spectrum of the (2000,A_1/F_2) band appears as a parallel band of a symmetric top, which is a further indication of the local mode character of stannane. The measurement and the analysis of the high-resolution infrared spectrum of both (2000,A_1/F_2) and (3000,A_1/F_2) bands of $^{116}SnH_4$ are now in progress in order to obtain information about local mode effects on the rotational energy level structure.

Acknowledgment. L.H. thanks the Academy of Finland for financial support. H.B. acknowledges financial support by the Fonds der Chemie.

Registry No. $^{116}SnH_4$, 105855-10-5; D, 7782-39-0.

Spectroscopic Detection of Ozone–Olefin Charge-Transfer Complexes in Cryogenic Matrices

Karen A. Singmaster*

Department of Chemistry, San Jose State University, San Jose, California 95192

and George C. Pimentel†

Laboratory of Chemical Dynamics, Lawrence Berkeley Laboratory, University of California, Berkeley, California 94720 *(Received: November 20, 1989)*

When ozone–olefin mixtures are codeposited in argon or krypton matrices, broad intense visible–UV absorptions appear that are clearly due to the long-sought ozone–olefin charge-transfer (C-T) complexes. With olefins tetramethylethylene, trimethylethylene, *cis*- and *trans*-2-butene, isobutylene, and propene, the maximum absorptions appear, respectively, at 500, 388, 400, 407, 388, and 345 nm. As is usual for C-T absorptions, these wavelengths provide values of ν_{max}(C-T) that correlate with the olefin ionization potentials. As the matrix temperature is raised, ozonolysis begins; kinetic measurements give activation energies of 1.0 ± 0.4 kcal/mol for the krypton matrix reaction between ozone and *cis*- or *trans*-2-butene. Other spectral characteristics provide evidence about the transient state of the complex after excitation in a vertical transition: its instantaneous dipole moment (~17 D) and its lifetime (~1–10 ps). In addition, rough measurements of the 0–0 transitions point to strong bonds in the equilibrium geometry of the excited-state complex.

Introduction

The possible existence of ozone–olefin charge-transfer (C-T) complexes has been a controversial subject, complicated by the ease of reaction of ozone with olefins to form ozonides. In the most recent work, Nelander and Nord[1] used matrix isolation techniques to show that earlier claims of detection of such complexes[2,3] were either due to ozonolysis reaction products[2] or due to trapped ozone.[3] They went on to search unsuccessfully for visible–UV absorptions that could be attributed to ozone–olefin complexes. The olefins they investigated included propene, *cis*- and *trans*-2-butene, and trimethylethylene in solid CO_2 at 95 K.

Aromatic–ozone C-T complexes are well-known from the work by Bailey and co-workers[4,5] using isopentane glasses at 195 °C. More recently, Hashimoto and Akimoto have reported UV absorptions attributable to O_2–olefin C-T complexes.[6] Both the O_3–aromatic and O_2–olefin spectral features show the traditional correlations between absorption maxima and ionization potentials and suggest that the olefins should also form such charge-transfer complexes with ozone provided that ozonolysis reactions can be prevented. Using cryogenic matrices of argon, krypton, and xenon, we have conclusive evidence for such charge transfer, as presented below.

Experimental Section

Matrices were deposited onto a CsI window cooled by Displex CSA-202 (Air Products and Chemicals, Inc.) closed-cycle helium refrigerator. Matrix mixtures were deposited at rates of 0.5 to

† Deceased. This paper is dedicated to Dr. Pimentel.

(1) Nelander, B.; Nord, L. *J. Am. Chem. Soc.* **1979**, *101*, 3769.
(2) Alcock, W. A.; Mile, B. *J. Chem. Soc., Chem. Commun.* **1976**, *5*.
(3) Hull, L. A.; Hisatsune, I. C.; Heicklen, J. *J. Am. Chem. Soc.* **1972**, *94*, 4856.
(4) Bailey, P. S.; Carter, T. P.; Nick, E.; Fisher, C. M.; Khasbal, A. Y. *J. Am. Chem. Soc.* **1974**, *96*, 6138.
(5) Bailey, P. S.; Ward, J. W.; Hornish, R. E. *J. Am. Chem. Soc.* **1971**, *93*, 3552.
(6) Hashimoto, S.; Akimoto, H. *J. Phys. Chem.* **1987**, *91*, 1347–1354.

0022-3654/90/2094-5226$02.50/0